Table 4. Cox Proportional Hazards Regression Analysis of the Association Between Primary Tumor Site and Event-Free and Overall Survival Without (unadjusted HR) and With Adjustment (adjusted HR) for Age at Diagnosis, *MYCN* Status, and INSS Stage

	Unadjusted			Adjusted		
Primary Tumor Site	HR	95% CI	*P*	HR	95% CI	*P*
			Event-Free Survival			
Adrenal	1	Ref	Ref	1	Ref	Ref
Abdominal/retroperitoneal	0.75	0.69 to 0.83	< .001	0.94	0.85 to 1.04	.225
Neck	0.40	0.30 to 0.54	< .001	0.98	0.70 to 1.36	.886
Thoracic	0.39	0.34 to 0.45	< .001	0.76	0.64 to 0.89	.001
Pelvic	0.39	0.29 to 0.51	< .001	0.89	0.64 to 1.24	.503
Other	0.75	0.65 to 0.87	< .001	0.85	0.72 to 1.02	.079
Nonadrenal	1	Ref	Ref	1	Ref	Ref
Adrenal	1.67	1.55 to 1.80	< .001	1.13	1.03 to 1.23	.008
Nonthoracic	1	Ref	Ref	1	Ref	Ref
Thoracic	0.46	0.40 to 0.52	< .001	0.79	0.67 to 0.92	.003
			Overall Survival			
Adrenal	1	Ref	Ref	1	Ref	Ref
Abdominal/retroperitoneal	0.70	0.63 to 0.77	< .001	0.94	0.84 to 1.06	.313
Neck	0.21	0.14 to 0.33	< .001	0.54	0.31 to 0.94	.029
Thoracic	0.28	0.24 to 0.33	< .001	0.65	0.52 to 0.80	< .001
Pelvic	0.20	0.13 to 0.30	< .001	0.65	0.39 to 1.07	.090
Other	0.70	0.59 to 0.83	< .001	0.86	0.70 to 1.06	.157
Nonadrenal	1	Ref	Ref	1	Ref	Ref
Adrenal	1.97	1.81 to 2.14	< .001	1.17	1.05 to 1.29	.003
Nonthoracic	1	Ref	Ref	1	Ref	Ref
Thoracic	0.34	0.29 to 0.40	< .001	0.68	0.56 to 0.84	< .001

Abbreviations: HR, hazard ratio; INSS, International Neuroblastoma Staging System; Ref, reference.

our knowledge, our finding that more thoracic tumors were diagnosed before 1996 is novel, and may reflect the impact of earlier NB screening efforts that identified a higher proportion of patients with favorable disease.[17,18] Previous studies have shown that the pelvic primary site in NB is a favorable location, with lower rates of *MYCN* amplification and advanced stage than nonpelvic primary tumor sites.[6,7] Given the rarity of occurrence, previous studies of primary NBs of the neck and cervical region are limited to small case series that suggest that favorable clinical and biologic features are also associated with these tumors, including lower-stage disease and less *MYCN* amplification.[19,20] To date, there are no indications that molecular events involved in tumorigenesis are distinct in NB according to primary site, although no genomic studies comparing DNA mutations by primary site have been performed.

It is known that *MYCN*-amplified NBs are characterized by highly aggressive behavior with unfavorable outcome. Perhaps the most striking biologic difference observed in the current study was in the proportion of *MYCN* amplification across primary tumor sites. Although other groups have reported such differences, we show for the first time, to our knowledge, that the substantially different rates of *MYCN* amplification according to primary tumor site are independent of other factors associated with *MYCN* amplification, including age, stage, and grade of differentiation. It is not clear whether developing neuroblasts in the adrenal medulla might be more susceptible to amplification at the *MYCN* locus or if our findings simply reflect a greater number of cells at risk for undergoing *MYCN* amplification at that site because of its size compared with other sympathetic tissues.

We also confirmed previous smaller analyses that demonstrated differences in outcomes according to primary site. For example, the superior unadjusted EFS and OS rates of thoracic primary tumors found in this study (80.0% and 87.6%, respectively) are comparable with those seen in single-center or cooperative group studies with overall survival rates ranging from 71.2% to 100%.[8,15,16,21] The biologically favorable profile of thoracic tumors may explain the better prognosis in these tumors. In one study, *MYCN*-amplified tumors with a thoracic primary were shown to have a better outcome compared with all nonthoracic NB tumors in a previous univariable survival analysis; however, a multivariable Cox analysis was not conducted in that study.[16] A key advantage of our study is our ability to control for potential confounding variables that might be associated both with primary tumor site and prognosis. As the largest multivariable analysis addressing the prognostic impact of primary tumor site, our study demonstrated that the inferior outcomes for patients with adrenal tumors and the superior outcomes for patients with thoracic and neck tumors are independent of differences in age, stage, and *MYCN* status associated with these sites. Interestingly, patients with neck tumors were at decreased risk of death, but not at decreased risk of an analytic event. One reason for this finding may be that, whereas cervical and cervicothoracic NBs have favorable prognostic features, their anatomic localization makes it difficult to completely resect them in many patients, and these tumors tend to recur locally.[19,22-24]

We have confirmed that primary tumor site plays an important role in the heterogeneity of NB. To address our aims, we used the INRG database to evaluate the largest available cohort of patients with NB. However, there are several limitations to analyzing data from a tumor registry. We were limited to the available variables in the registry. As such, we were unable to report on important variables, such as extent of surgery and chemotherapy/radiation treatment used. Although we were able to describe the frequency of stage 3 disease by primary site, we were not able to assess whether a patient was deemed

to have stage 3 disease because of tumor crossing the midline, contralateral node involvement, or both. In addition, we were unable to confirm the primary tumor site designation of the "other" category, which may represent rare primary tumor sites, multifocal primary tumors, large tumors that may cross two or more anatomic compartments, or tumors of unknown origin. Along these lines, some large so-called abdominal/retroperitoneal tumors may have had ambiguous origins and may have actually arisen from adjacent adrenal or pelvic sites. It should be noted that the INRG database contains data from multiple cooperative groups, and it is possible that some patients who were included in our analysis were reported in previous studies on this topic. In addition, contributing cooperative groups may have used slightly different definitions of sites of disease. Moreover, our classification of segmental chromosomal aberrations included only the LOH/aberration at 1p, gain of 17q, and 11q aberration. Our evaluation of these variables separately and also as a pooled variable may differ from previous smaller studies, but these genetic aberrations have been shown to have prognostic significance in previous INRG studies.[12,13] Finally, some clinical and biologic variables were missing for some patients, as noted in Tables 1 and 2, and we could only report on what was available in the INRG database.

On the basis of our findings, we conclude that there are statistically significant differences in clinical features, biologic characteristics, and outcomes between primary tumor sites in NB. Our results suggest that there is something distinctive about the tumor in these specific sites of origin that leads to or reflects different biology and clinical behavior. Further study of the developmental biology of the neural crest and sympathetic nervous system may elucidate the etiology for these observed differences. Likewise, additional efforts should be directed at elucidating the disordered mechanisms of embryonal tumorigenesis in NB.

AUTHORS' DISCLOSURES OF POTENTIAL CONFLICTS OF INTEREST

The author(s) indicated no potential conflicts of interest.

AUTHOR CONTRIBUTIONS

Conception and design: Kieuhoa T. Vo, Katherine K. Matthay, Wendy B. London, Steven G. DuBois
Administrative support: Wendy B. London
Collection and assembly of data: Kieuhoa T. Vo, Katherine K. Matthay, Wendy B. London, Barbara Hero, Peter F. Ambros, Akira Nakagawara, Andy D.J. Pearson, Susan L. Cohn, Steven G. DuBois
Data analysis and interpretation: Kieuhoa T. Vo, Katherine K. Matthay, John Neuhaus, Wendy B. London, Peter F. Ambros, Akira Nakagawara, Doug Miniati, Kate Wheeler, Andy D.J. Pearson, Susan L. Cohn, Steven G. DuBois
Manuscript writing: All authors
Final approval of manuscript: All authors

REFERENCES

1. Carlsen NL, Christensen IJ, Schroeder H, et al: Prognostic factors in neuroblastomas treated in Denmark from 1943 to 1980: A statistical estimate of prognosis based 253 cases. Cancer 58:2726-2735, 1986
2. Oppedal BR, Storm-Mathisen I, Lie SO, et al: Prognostic factors in neuroblastoma: Clinical, histopathologic, and immunohistochemical features and DNA ploidy in relation to prognosis. Cancer 62:772-780, 1988
3. Joshi VV, Cantor AB, Altshuler G, et al: Recommendations for modifications of terminology of neuroblastic tumors and prognostic significance of Shimada classification: A clinicopathologic study of 213 cases from the Pediatric Oncology Group. Cancer 69:2183-2196, 1992
4. Sung KW, Yoo KH, Koo HH, et al: Neuroblastoma originating from extra-abdominal sites: Association with favorable clinical and biological features. J Korean Med Sci 24:461-467, 2009
5. Ladenstein R, Urban C, Gadner H, et al: First experience with prognostic factors in unselected neuroblastoma patients: The Austrian Neuroblastoma 87 study. Eur J Cancer 31A:637-641, 1995
6. Haase GM, O'Leary MC, Stram DO, et al: Pelvic neuroblastoma: Implications for a new favorable subgroup: A Children's Cancer Group experience. Ann Surg Oncol 2:516-523, 1995
7. Leclair MD, Hartmann O, Heloury Y, et al: Localized pelvic neuroblastoma: Excellent survival and low morbidity with tailored therapy—The 10-year experience of the French Society of Pediatric Oncology. J Clin Oncol 22:1689-1695, 2004
8. Adams GA, Shochat SJ, Smith EI, et al: Thoracic neuroblastoma: A Pediatric Oncology Group study. J Pediatr Surg 28:372-378, 1993
9. Caron HN: Are thoracic neuroblastomas really different? Pediatr Blood Cancer 54:867, 2010
10. Cohn SL, Pearson AD, London WB, et al: The International Neuroblastoma Risk Group (INRG) classification system: An INRG Task Force report. J Clin Oncol 27:289-297, 2009
11. Shimada H, Ambros IM, Dehner LP, et al: Terminology and morphologic criteria of neuroblastic tumors: Recommendations by the International Neuroblastoma Pathology Committee. Cancer 86:349-363, 1999
12. Ambros PF, Ambros IM, Brodeur GM, et al: International consensus for neuroblastoma molecular diagnostics: Report from the International Neuroblastoma Risk Group (INRG) Biology Committee. Br J Cancer 100:1471-1482, 2009
13. Schleiermacher G, Mosseri V, London WB, et al: Segmental chromosomal alterations have prognostic impact in neuroblastoma: A report from the INRG project. Br J Cancer 107:1418-1422, 2012
14. Kaplan EL, Meier P: Nonparametric estimation from incomplete observations. J Am Stat Assoc 53:457-481, 1958
15. Häberle B, Hero B, Berthold F, et al: Characteristics and outcome of thoracic neuroblastoma. Eur J Pediatr Surg 12:145-150, 2002
16. Morris JA, Shcochat SJ, Smith EI, et al: Biological variables in thoracic neuroblastoma: A Pediatric Oncology Group Study. J Pediatr Surg 30:296-303, 1995
17. Schilling FH, Spix C, Berthold F, et al: Neuroblastoma screening at one year of age. N Engl J Med 346:1047-1053, 2002
18. Tanaka M, Kigasawa H, Kato K, et al: A prospective study of a long-term follow-up of an observation program for neuroblastoma detected by mass screening. Pediatr Blood Cancer 54:573-578, 2010
19. Qureshi SS, Kembhavi S, Ramadwar M, et al: Outcome and morbidity of surgical resection of primary cervical and cervicothoracic neuroblastoma in children: A comparative analysis. Pediatr Surg Int 30:267-273, 2014
20. Abramson SJ, Berdon WE, Ruzal-Shapiro C, et al: Cervical neuroblastoma in eleven infants: A tumor with favorable prognosis—Clinical and radiologic (US, CT, MRI) findings. Pediatr Radiol 23:253-257, 1993
21. Demir HA, Yalçin B, Büyükpamukçu N, et al: Thoracic neuroblastic tumors in childhood. Pediatr Blood Cancer 54:885-889, 2010
22. Matthay KK, Sather HN, Seeger RC, et al: Excellent outcome of stage II neuroblastoma is independent of residual disease and radiation therapy. J Clin Oncol 7:236-244, 1989
23. Cardesa-Salzmann TM, Mora-Graupera J, Claret G, et al: Congenital cervical neuroblastoma. Pediatr Blood Cancer 43:785-787, 2004
24. Haddad M, Triglia JM, Helardot P, et al: Localized cervical neuroblastoma: Prevention of surgical complications. Int J Pediatr Otorhinolaryngol 67: 1361-1367, 2003

Support

Supported in part by a Cancer Research UK Life Chair and Programme grant included within a Cancer Research UK Institute of Cancer Research (ICR) Core Award (No. C347/A15403; A.D.J.P.), the National Institute for Health Research Royal Marsden/ICR Biomedical Research Centre (A.D.J.P.), Alex's Lemonade Stand Foundation (K.T.V., K.K.M., S.G.D.), the Frank A. Campini Foundation (K.K.M., S.G.D.), the Edward Conner

Fund (K.K.M.), the Dougherty Foundation (K.K.M., S.G.D.), and the Mildred V. Strouss Chair (K.K.M.). The International Neuroblastoma Risk Group database is supported in part by the William Guy Forbeck Research Foundation, the Little Heroes Cancer Research Fund, the Children's Neuroblastoma Cancer Foundation, the Neuroblastoma Children's Cancer Foundation, and the Super Jake Foundation.

GLOSSARY TERMS

Cox proportional hazards regression model: a statistical model for regression analysis of censored survival data, examining the relationship of censored survival distribution to one or more covariates. This model produces a baseline survival curve, covariate coefficient estimates with their standard errors, risk ratios, 95% CIs, and significance levels.

event-free survival: calculated from the date of diagnosis to the date of the first event, which is resistance, relapse, death, or second malignant neoplasm.

logistic regression analysis: a multivariable regression model in which the log of the odds of a time-fixed outcome event (eg, 30-day mortality) or other binary outcome is related to a linear equation.

loss of heterozygosity (LOH): a situation in which one chromosome has a normal allele of a gene and one chromosome has a mutant or deleted allele.

MYCN: gene encoding for c-myc.

overall survival: the duration between random assignment and death.

Appendix

Table A1. Sites of Metastases of Patients With Stage 4 Neuroblastoma by Primary Tumor Site (n = 2,899)

			Primary Tumor Site												
	All (n = 2,899)		Adrenal (n = 1,773)		Abdominal/ Retroperitoneal (n = 628)		Neck (n = 38)		Thoracic (n = 258)		Pelvic (n = 34)		Other (n = 171)		
Metastatic Site	No.	%	No.	%	No.	%	No.	%	No.	%	No.	%	No.	%	*P**
Bone marrow	2,146	74	1,362	77	455	72	24	63	166	64	22	71	117	68	< .001
Bone	1,783	61	1,158	65	361	57	16	42	132	51	14	45	102	60	< .001
Distant lymph nodes	1,000	34	635	36	199	32	14	37	85	33	9	29	58	34	.499
Liver	514	18	359	20	100	16	3	8	27	10	3	10	22	13	< .001
Lung	99	3	68	4	22	3	0	0	3	1	1	3	5	3	.269
CNS	76	3	55	3	10	2	2	5	4	2	0	0	5	3	.199
Skin	80	3	48	3	15	2	1	3	7	3	0	0	9	5	.390
Other	820	28	520	29	143	23	11	29	72	28	9	29	65	38	.003

*P value refers to χ^2 test.

AACR American Association for Cancer Research

Clinical Cancer Research

Revised risk estimation and treatment stratification of low- and intermediate-risk neuroblastoma patients by integrating clinical and molecular prognostic markers

Andre Oberthuer, Dilafruz Juraeva, Barbara Hero, et al.

Clin Cancer Res Published OnlineFirst September 17, 2014.

Biochemical and Biophysical Research Communications 453 (2014) 86–93

Contents lists available at ScienceDirect

Biochemical and Biophysical Research Communications

journal homepage: www.elsevier.com/locate/ybbrc

Intracellular fragment of NLRR3 (NLRR3-ICD) stimulates ATRA-dependent neuroblastoma differentiation

Jesmin Akter [a], Atsushi Takatori [b,*], Md. Sazzadul Islam [a], Atsuko Nakazawa [c], Toshinori Ozaki [d,*], Hiroki Nagase [b], Akira Nakagawara [e]

[a] Laboratory of Innovative Cancer Therapeutics, Chiba Cancer Center Research Institute, Chiba 260-8717, Japan
[b] Laboratory of Cancer Genetics, Chiba Cancer Center Research Institute, Chiba 260-8717, Japan
[c] Department of Pathology, National Center for Child Health and Development, Tokyo, Japan
[d] Laboratory of DNA Damage Signaling, Chiba Cancer Center Research Institute, Chiba 260-8717, Japan
[e] Saga Medical Centre, 840-8571, Japan

ARTICLE INFO

Article history:
Received 13 September 2014
Available online 23 September 2014

Keywords:
ATRA
Differentiation
Neuroblastoma
NLRR3
Secretase

ABSTRACT

We have previously identified neuronal leucine-rich repeat protein-3 (NLRR3) gene which is preferentially expressed in favorable human neuroblastomas as compared with unfavorable ones. In this study, we have found for the first time that NLRR3 is proteolytically processed by secretases and its intracellular domain (NLRR3-ICD) is then released to translocate into cell nucleus during ATRA-mediated neuroblastoma differentiation. According to our present observations, NLRR3-ICD was induced to accumulate in cell nucleus of neuroblastoma SH-SY5Y cells following ATRA treatment. Since the proteolytic cleavage of NLRR3 was blocked by α- or γ-secretase inhibitor, it is likely that NLRR3-ICD is produced through the secretase-mediated processing of NLRR3. Intriguingly, forced expression of NLRR3-ICD in neuroblastoma SK-N-BE cells significantly suppressed their proliferation as examined by a live-cell imaging system and colony formation assay. Similar results were also obtained in neuroblastoma TGW cells. Furthermore, overexpression of NLRR3-ICD stimulated ATRA-dependent neurite elongation in SK-N-BE cells. Together, our present results strongly suggest that NLRR3-ICD produced by the secretase-mediated proteolytic processing of NLRR3 plays a crucial role in ATRA-mediated neuronal differentiation, and provide a clue to develop a novel therapeutic strategy against aggressive neuroblastomas.

1. Introduction

Neuroblastoma which originates from the sympathetic nervous system during embryogenesis, is the most common extra cranial solid tumor in children, accounting for 15% of childhood cancer deaths [1]. Neuroblastoma is highly heterogeneous, and thus characterized by a wide variety of its clinical behaviors, from spontaneous regression to aggressive progression. For example, tumors found in infants less than 1 year of age frequently regress through the spontaneous differentiation and/or apoptosis, resulting in a favorable prognosis [2]. It has been shown that neuroblastoma cells with better prognosis are often found to express various prognostic markers indicative of cell differentiation, such as *HNK-1* or *TrkA* [3,4]. On the other hand, around 40% of the patients diagnosed with neuroblastoma are included in the high-risk category based on prognostic indicators such as age at diagnosis, stage, tumor histology, proto-oncogene *MYCN* status, and DNA ploidy [5,6]. Among them, the poor clinical outcome and aggressive tumor phenotype of high-risk neuroblastoma strongly correlate with the amplification of *MYCN* and enhanced tumor angiogenesis [7]. Although patients with the high-risk tumors usually have a good immediate response to the standard treatment, the majority of them frequently acquire resistance to the therapy with fatal outcome [1]. Therefore, a novel strategy to treat these advanced tumors is highly required.

Intriguingly, neuroblastoma cells display the similar characteristics to undifferentiated cells [8], indicating that the tumorigenesis of neuroblastoma results from defect in differentiation of embryonic neural crest progenitor cells [9]. With this in mind, a growing body of evidence strongly suggests that neuroblastoma cells have an ability to differentiate into mature cells and can be

* Corresponding authors at: Laboratory of Cancer Genetics, Chiba Cancer Center Research Institute, 666-2 Nitona, Chuoh-ku, Chiba 260-8717, Japan. Fax: +81 43 265 4459 (A. Takatori). Laboratory of DNA Damage Signaling, Chiba Cancer Center Research Institute, 666-2 Nitona, Chuoh-ku, Chiba 260-8717, Japan. Fax: +81 43 265 4459 (T. Ozaki).

E-mail addresses: atakatori@chiba-cc.jp (A. Takatori), tozaki@chiba-cc.jp (T. Ozaki).

http://dx.doi.org/10.1016/j.bbrc.2014.09.065
0006-291X/

forced to differentiate in response to retinoic acid (RA) [10]. RA has been shown to play an important role in early embryonic development and in the generation of several systems such as nervous system [11]. Based on these findings, RA-mediated terminal differentiation of neuroblastoma is used as a current standard therapy for the high-risk neuroblastoma, however, a precise molecular basis underlying neuroblastoma differentiation has been elusive.

To understand a molecular mechanism(s) behind the genesis as well as the aggressive progression of neuroblastoma, we have identified a large number of genes expressed differentially between favorable and unfavorable neuroblastomas [12]. NLRR3 is one of NLRR family of type I transmembrane protein with the typical leucine-rich repeat (LRR) domain, and its expression level was extremely higher in favorable neuroblastomas than that in unfavorable ones, indicating that *NLRR3* expression might be one of favorable prognostic indicators in neuroblastoma [12,13]. Recently, we have found that MYCN has an ability to repress the transcription of *NLRR3* through the functional collaboration with Miz-1, raising a possibility that MYCN-induced down-regulation of NLRR3 contributes at least in part to the aggressive phenotype of the high-risk neuroblastoma [14]. However, the precise molecular event(s) and mechanism(s) involved remain unclear.

In this study, we have found that the intracellular fragment of NLRR3 (NLRR3-ICD) plays a pivotal role in the regulation of ATRA (all-*trans* retinoic acid)-mediated neuroblastoma differentiation.

2. Materials and methods

2.1. Cell lines

Human neuroblastoma SK-N-BE, SH-SY5Y and TGW cells were grown in RPMI 1640 medium (Sigma) supplemented with 10% heat-inactivated fetal bovine serum (Invitrogen), 100 units/ml of penicillin and 100 μg/ml of streptomycin. Cells were grown at 37 °C in a humidified incubator with 5% CO_2. For neuroblastoma differentiation experiments, SH-SY5Y cells were exposed to 5 μM of all-*trans* retinoic acid (ATRA; Sigma).

2.2. Clinical samples

Patient samples were collected with patients' written informed consent in accordance with ethics approval obtained from the internal review board.

2.3. Transfection

Cells were transfected with the indicated expression plasmids using LipofectAMINE 2000 (Invitrogen) according to the manufacturer's instructions.

2.4. Deletion constructs of NLRR3

The expression plasmids encoding human NLRR3 (1–708), NLRR3-ECD (1–649), NLRR3-ECD-sol (1–628), NLRR3-d-ECD (629–708) or NLRR3-ICD (648–708) were generated by PCR-based amplification. PCR products were gel-purified and inserted into the appropriate restriction sites of pcDNA3.1 expression plasmid (Invitrogen) with COOH-terminal HA epitope tag to give pcDNA3.1-NLRR3, pcDNA3.1-NLRR3-ECD, pcDNA3.1-NLRR3-ECD-sol, pcDNA3.1-NLRR3-d-ECD and pcDNA3.1-NLRR3-ICD. The nucleotide sequences of these expression plasmids were verified by DNA sequencing.

2.5. Cell survival assay

Cells were seeded at a density of 1.0×10^3 cells/96-well plates and allowed to attach overnight. Cells were then maintained in standard culture medium, and visualized using a real-time cell imaging system (IncuCyte; Essen's Bioscience) according to the manufacturer's recommendations.

2.6. Colony formation assay

SK-N-BE or TGW cells were seeded at a density of 2.0×10^3 -cells/6-well plates, and then transfected with the indicated expression plasmids. Forty-eight hours after transfection, cells were transferred to the fresh medium containing G418 (600 μg/ml). After 14 days of the incubation, G418-resistant colonies were fixed in methanol, and stained with Giemsa's solution.

2.7. Immunoprecipitation

Equal amounts of cell lysates (1 mg of protein) were precleared with 20 μl of protein A-Sepharose beads (GE Healthcare) and subjected to immunoprecipitation with anti-NLRR3 or with anti-HA antibody (Roche). The immunoprecipitates were then analyzed by immunoblotting with anti-NLRR3 or with anti-HA antibody. ECL (enhanced chemiluminescence; GE Healthcare) was used to detect the presence of immuno-reactive bands.

2.8. Immunohistochemistry

Paraffin-embedded sympathetic ganglia tissues were fixed in 10% formaldehyde and then incubated with anti-NLRR3 antibody. Immunohistochemical analysis was performed as described [14].

2.9. Immunofluorescence

Cells were grown on glass coverslips in standard culture medium. Cells were washed in PBS, fixed in 4% paraformaldehyde for 20 min at 4 °C, permeabilized with 0.1% Triton X-100 for 20 min at room temperature, and then blocked with 1% BSA plus 5% goat serum for 1 h at room temperature. After blocking, cells were incubated with anti-HA, anti-NLRR3, anti-Tuj-1 antibody (Covance) or with a normal rabbit IgG for 1 h at room temperature, followed by the incubation with Alexa Fluor 546-conjugated goat anti-rabbit IgG (Life Technologies). Cell nuclei were stained with DAPI. The coverslips were mounted into glass slides, and images were captured using a confocal laser scanning microscope (Leica).

2.10. Statistical analysis

All values were expressed as the means ± SEM. One-way ANOVA with a post hoc Dunnett's test were used to determine level of significance for colony formation assay and percentage of differentiated cells ($^{**}P < 0.01$). Two-way ANOVA followed by a multiple comparison post hoc Bonferroni's test was used to compare differences between groups in cell viability assay ($^{*}P < 0.05$ and $^{**}P < 0.01$).

3. Results

3.1. Induction of NLRR3-related peptide during ATRA-mediated neuroblastoma differentiation

To examine the expression pattern of NLRR3 during ATRA (all-*trans* retinoic acid)-dependent neuroblastoma differentiation, human neuroblastoma SH-SY5Y cells were exposed to 5 μM of

ATRA. At the indicated time periods after treatment, cell lysates were subjected to immunoprecipitation/immunoblotting with anti-NLRR3 antibody. Consistent with our recent findings [14], an obvious elongation of neurite (one of the hallmark processes of neuronal morphological differentiation) was observed in ATRA-treated SH-SY5Y cells in a time-dependent manner (Fig. 1A). It is worth noting that ATRA promotes a remarkable accumulation of a small peptide which is recognized by anti-NLRR3 antibody (Fig. 1B).

Since anti-NLRR3 antibody was raised against the extreme COOH-terminal intracellular domain of NLRR3 [14], it is possible that, like NICD (Notch intracellular domain) [15], this small peptide is produced by a proteolytic cleavage of NLRR3 in SH-SY5Y cells exposed to ATRA. It has been well-documented that, upon ligand binding, NICD is released from the plasma membrane after proteolytic processing, and thereby translocating into cell nucleus [15]. To test this possibility, we performed the indirect immunofluorescence experiments to examine the subcellular localization of NLRR3 in response to ATRA. At the indicated time points after ATRA treatment, SH-SY5Y cells were fixed and stained with anti-NLRR3 antibody. As shown in Fig. 1C, NLRR3 was extremely detectable outside of cell nucleus in the absence of ATRA. Intriguingly, a small fraction of NLRR3 was clearly induced to accumulate in ATRA-treated cell nucleus in a time-dependent fashion, suggesting that ATRA-mediated proteolysis releases the intracellular domain of NLRR3 from plasma membrane and thereby promoting its nuclear access. Although further experiments should be required to address this issue, we tentatively termed this small peptide NLRR3-ICD (NLRR3 intracellular domain).

3.2. Secretase-dependent proteolytic cleavage of NLRR3 to generate NLRR3-ICD

It has been widely accepted that NICD is generated through the sequential and highly regulated intramembrane proteolysis mediated by three distinct types of proteases including γ-secretase complex [15]. As described [16], γ-secretase cleaves quite a broad range of substrates, and there are no distinct consensus amino acid sequences of intramembrane γ-cleavage sites among them (Fig. 2A). Considering that NLRR3-ICD might be released from the plasma membrane, it is likely that γ-secretase-mediated proteolytic cleavage is involved in the production of NLRR3-ICD. To verify this hypothesis, we took advantage of γ-secretase inhibitor, inhibitor X [17]. SH-SY5Y cells were treated with inhibitor X or left untreated. Twenty-four hours post treatment, cell lysates were analyzed by immunoprecipitation/immunoblotting with anti-NLRR3 antibody. As shown in Fig. 2B, NLRR3-ICD was undetectable in the presence of inhibitor X, indicating that γ-secretase activity is required for the production of NLRR3-ICD.

To further confirm this issue, neuroblastoma SK-N-BE cells were transfected with the expression plasmid for HA-tagged NLRR3, followed by an incubation with or without inhibitor X. The endogenous expression level of NLRR3 in SK-N-BE cells was quite low when compared with that in SH-SY5Y cells (data not shown).

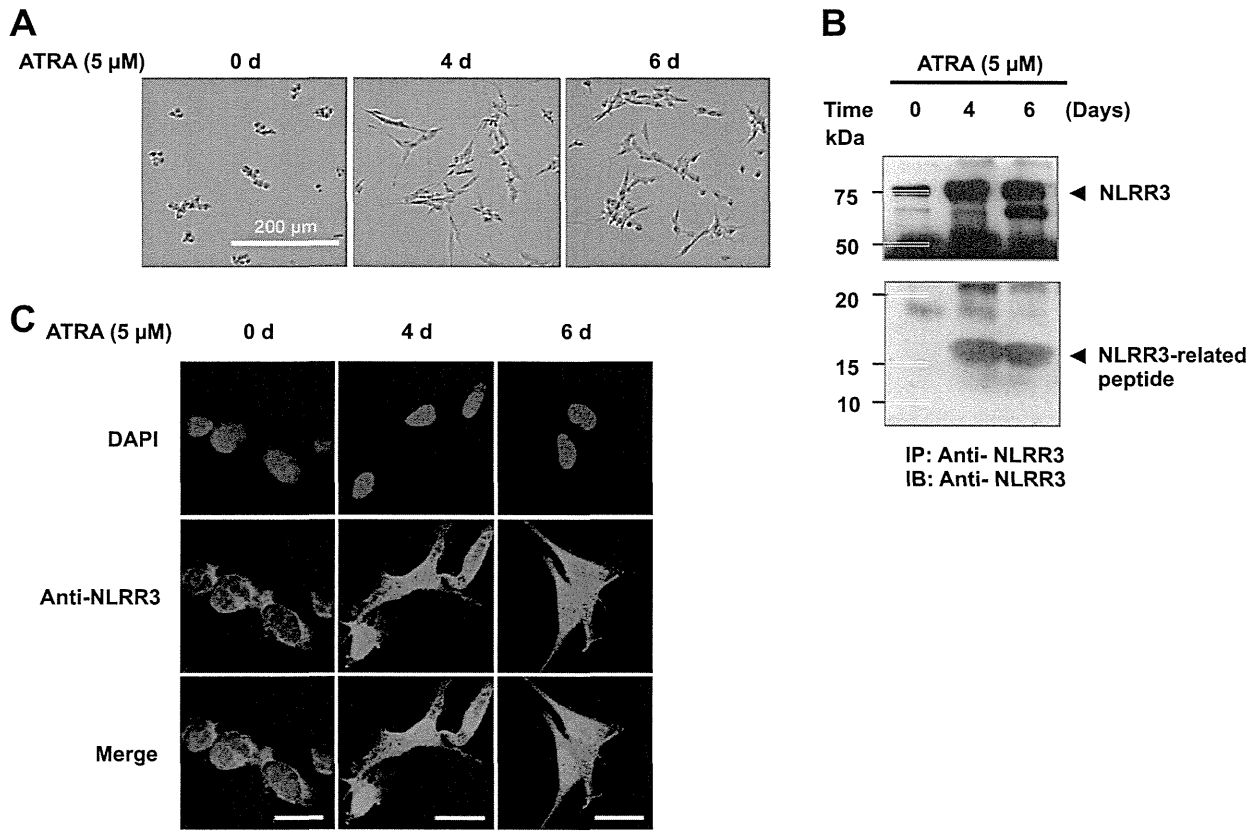

Fig. 1. Accumulation of an NLRR3-related peptide during ATRA-mediated neuroblastoma differentiation. (A) ATRA-mediated neuronal differentiation of neuroblastoma SH-SY5Y cells. SH-SY5Y cells were treated with 5 μM of ATRA. At the indicated time periods after treatment, pictures were taken. Note that ATRA-dependent neurite outgrowth was seen. Scale bar; 200 μm. (B) Expression of NLRR3 in response to ATRA. SH-SY5Y cells were treated as in (A). At the indicated time points after ATRA exposure, cell lysates were analyzed by immunoprecipitation with anti-NLRR3 antibody, followed by immunoblotting with anti-NLRR3 antibody. Arrow heads indicate native NLRR3 and NLRR3-related peptide. (C) ATRA-mediated nuclear access of NLRR3. SH-SY5Y cells were treated as in (A). At the indicated time periods after ATRA treatment, cells were fixed and then probed with anti-NLRR3 antibody, followed by the incubation with Alexa flour 546-conjugated secondary antibody (red). Cells were also stained with DAPI to visualize nuclei (blue). Scale bar; 25 μm. (For interpretation of the references to color in this figure legend, the reader is referred to the web version of this article.)

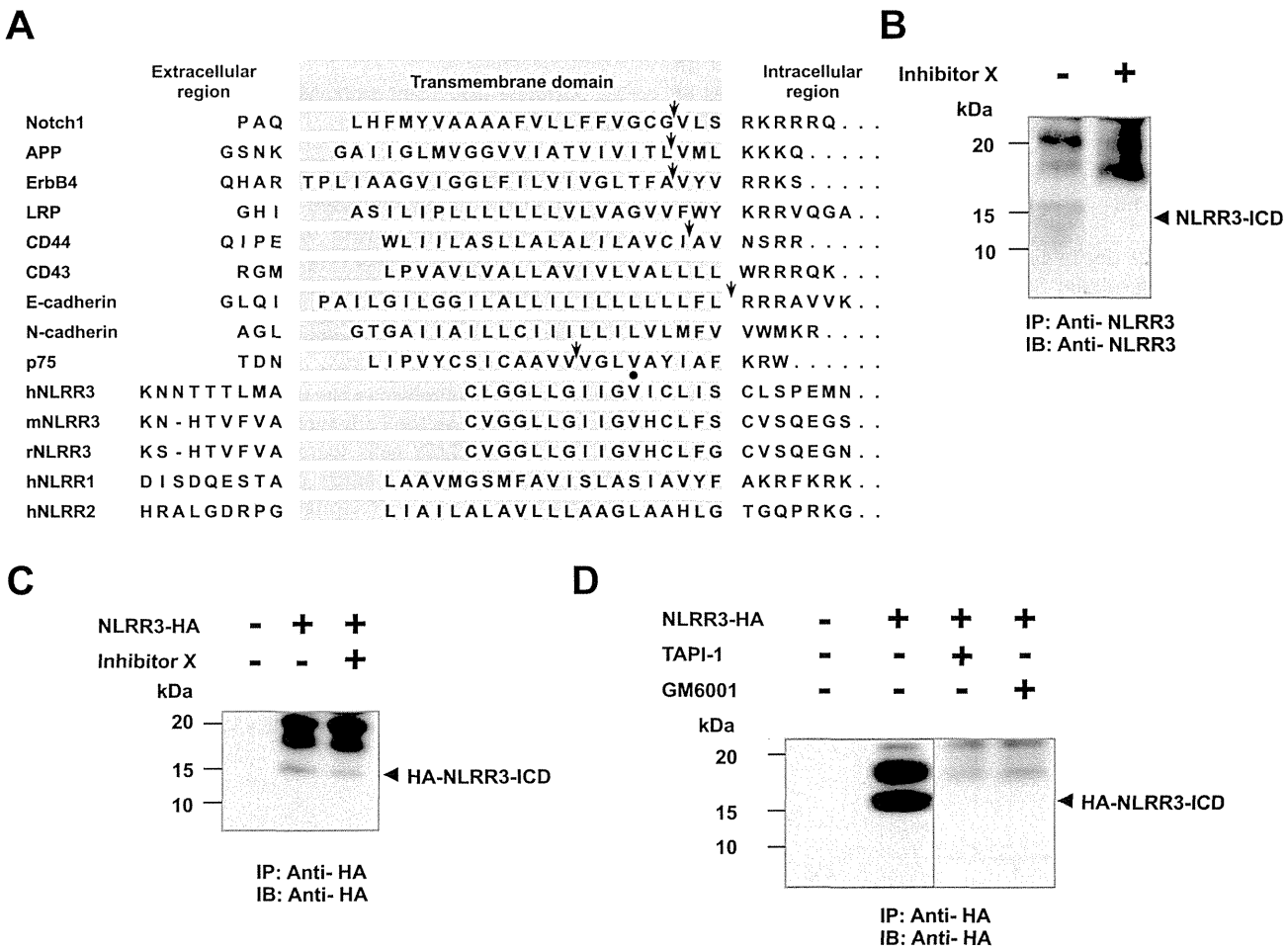

Fig. 2. Production of NLRR3 COOH-terminal peptide (NLRR3-ICD) through the proteolytic cleavage of NLRR3 by α- and γ-secretases. (A) Alignment of the amino acid sequences from transmembrane domains of human γ-secretase substrates. Arrows and filled circle indicate γ-cleavage sites of the indicated substrates and potential γ-cleavage site of NLRR3, respectively. (B and C) γ-secretase inhibitor blocks the production of NLRR3-ICD. SH-SY5Y cells were treated with 1 μM of inhibitor X or left untreated. Twenty-four hours after treatment, cell lysates were immunoprecipitated with anti-NLRR3 antibody, followed by immunoblotting with anti-NLRR3 antibody (B). SK-N-BE cells were transfected with the empty plasmid or with the expression plasmid for HA-NLRR3 and treated with or without inhibitor X. Twenty-four hours after treatment, cell lysates were subjected to immunoprecipitation with anti-HA antibody, followed by immunoblotting with anti-HA antibody (C). (D) The production of NLRR3-ICD is blocked by α-secretase inhibitors. SK-N-BE cells were transfected with the empty plasmid or with the expression plasmid encoding HA-NLRR3, and incubated in the presence or absence of TAPI-1 (20 μM) or GM6001 (10 μM). Twenty-four hours after treatment, cell lysates were processed for immunoprecipitation with anti-HA antibody, followed by immunoblotting with anti-HA antibody.

Twenty-four hours after treatment, cell lysates were analyzed by immunoprecipitation/immunoblotting with anti-HA antibody. As shown in Fig. 2C, the amount of HA-NLRR3-ICD was reduced in cells exposed to inhibitor X. Next, we have introduced the expression plasmid encoding HA-NLRR3 into SK-N-BE cells, and the transfected cells were then exposed to α-secretase inhibitors such as TAPI-1 and GM6001 [18] or left untreated. As clearly seen in Fig. 2D, the generation of HA-NLRR3-ICD was greatly abolished by these inhibitor treatments. Thus, it is highly likely that NLRR3-ICD is produced at least in part through the secretase-dependent proteolytic cleavage of NLRR3.

3.3. Nuclear access of NLRR3-ICD

We next assessed whether NLRR3-ICD could be localized within cell nucleus. SK-N-BE cells were transfected with the expression plasmid for HA-NLRR3. Forty-eight hours post transfection, the transfected cells were biochemically fractionated into cytoplasmic and nuclear fractions, and equal amounts of each fraction were analyzed by immunoblotting with anti-HA antibody. The purity of the cytoplasmic and nuclear fractions were verified by immunoblotting with anti-tubulin-α and anti-lamin B antibodies, respectively. As shown in Fig. 3A, the exogenously expressed HA-NLRR3 underwent proteolytic processing and the resultant HA-NLRR3-ICD was largely detected in nuclear fraction.

To gain further insights into the nuclear distribution of NLRR3-ICD, we have constructed the expression plasmids encoding the indicated HA-NLRR3 deletion mutants (Fig. 3B), and introduced them into SK-N-BE cells. Forty-eight hours after transfection, cells were fixed and probed with anti-HA antibody. As shown in Fig. 3C, HA-NLRR3-ECD and HA-NLRR3-ECD-sol lacking the intracellular domain of NLRR3, exclusively existed outside of cell nucleus, whereas HA-NLRR3-d-ECD containing NLRR3 intracellular domain, was found in both cytoplasm and nucleus. As expected, the nuclear distribution of HA-NLRR3-ICD was observed under our experimental conditions.

Next, we sought to examine whether the nuclear NLRR3 could be also detectable *in vivo*. For this purpose, we have performed an immunohistochemical analysis. Human sympathetic ganglia were fixed in formaldehyde, followed by an incubation with normal rabbit serum or with anti-NLRR3 antibody. As shown in Fig. 3D, anti-NLRR3 antibody recognized the nuclear NLRR3 in sympathetic ganglia, whereas normal rabbit serum did not detect any signals. Together, it appears that NLRR3 is subjected to the

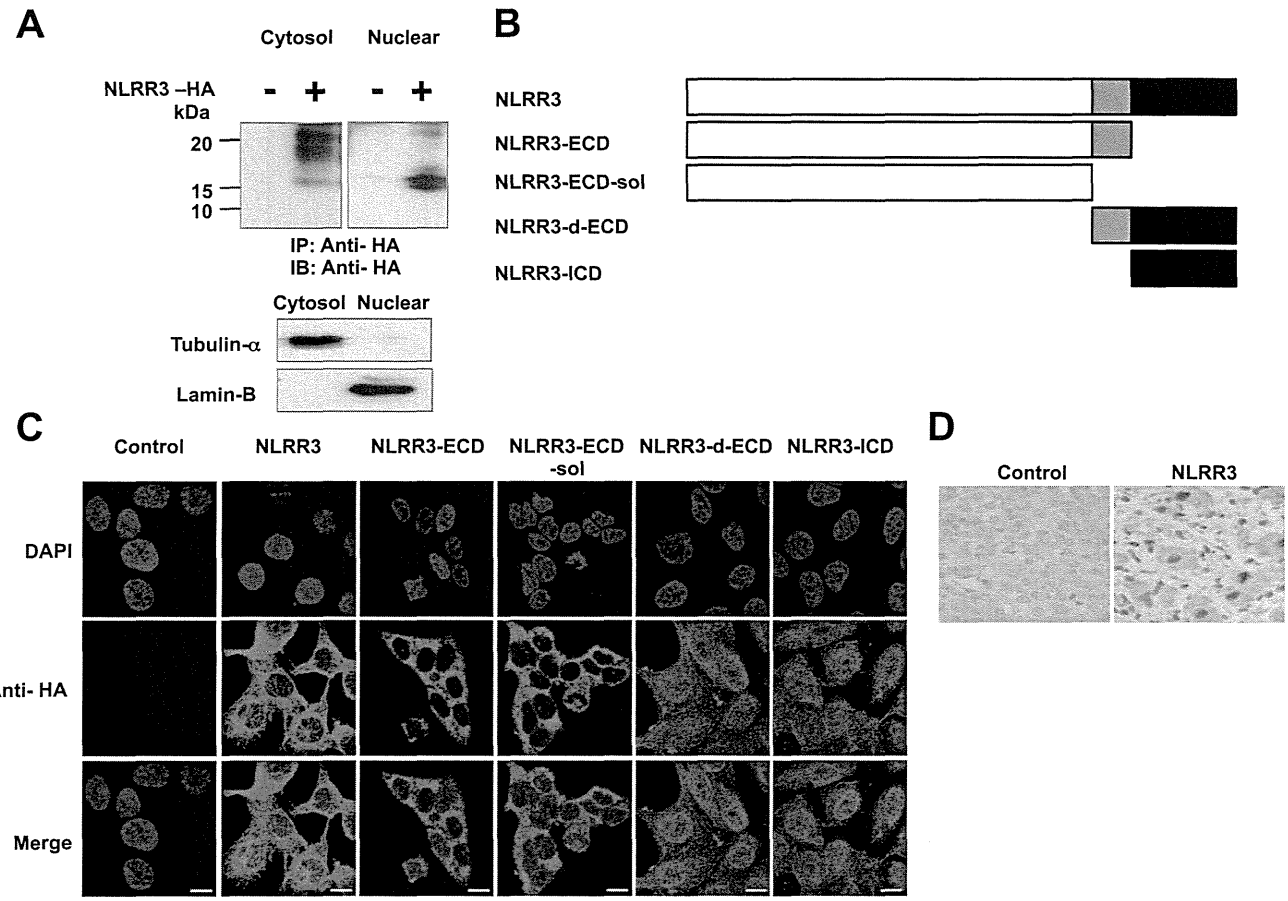

Fig. 3. Nuclear localization of NLRR3-ICD in neuroblastoma cells. (A) Immunoblotting. SK-N-BE cells were transfected with the empty plasmid or with the expression plasmid for HA-NLRR3. Forty-eight hours after transfection, cells were fractionated into cytoplasmic (C) and nuclear (N) fractions. Equal amounts of each fraction were analyzed by immunoblotting with anti-HA (upper panels), anti-Tubulin-α (middle panel), or with anti-Lamin B (lower panel). (B) Schematic diagrams of a full-length NLRR3 and its deletion mutants. Extracellular, transmembrane and intracellular domains of NLRR3 are indicated by open, gray and filled boxes, respectively. (C) Nuclear access of NLRR3-ICD. SK-N-BE cells were transfected with the expression plasmids encoding the above-mentioned HA-NLRR3 derivatives. Forty-eight hours after transfection, cells were fixed and stained with anti-HA antibody (red). Cell nuclei were stained with DAPI (blue). Scale bar; 10 μm. (D) Immunohistochemical staining. Human sympathetic ganglia were incubated with control IgG (left panel) or with anti-NLRR3 antibody (right panel). (For interpretation of the references to color in this figure legend, the reader is referred to the web version of this article.)

proteolytic processing, and thereby translocated from cell membrane to cell nucleus of cultured neuroblastoma cells as well as sympathetic ganglia.

3.4. NLRR3-ICD suppresses neuroblastoma cell proliferation

To explore a possible biological role(s) of NLRR3-ICD, we have examined the effect(s) of the indicated HA-NLRR3 derivatives including HA-NLRR3-ICD on neuroblastoma cell proliferation. SK-N-BE cells stably expressing the indicated HA-NLRR3 derivatives were cultured and their proliferation was monitored by IncuCyte live-cell imaging system. As shown in Fig. 4A, HA-NLRR3, HA-NLRR3-d-ECD and HA-NLRR3-ICD significantly suppressed SK-N-BE cell proliferation as compared with their parental cells. In a sharp contrast, HA-NLRR3-ECD and HA-NLRR3-ECD-sol had an undetectable effect on the rate of proliferation of SK-N-BE cells.

To further evaluate these observations, we have performed colony formation assay. SK-N-BE cells transfected with the indicated HA-NLRR3 derivatives were transferred to the fresh medium containing G418 (600 μg/ml). Two weeks after selection, number of drug-resistant colonies was scored. As shown in Fig. 4B and C, overexpression of HA-NLRR3-d-ECD or HA-NLRR3-ICD resulted in a remarkable decrease in number of drug-resistant colonies as compared with the empty plasmid control cells, whereas HA-NLRR3-ECD and HA-NLRR3-ECD-sol had a marginal effect on number of drug-resistant colonies. Additionally, cells overexpressing HA-NLRR3 showed a modest decrease in the rate of colony formation. Similar results were also obtained in neuroblastoma TGW cells (data not shown). Thus, these results indicate that NLRR3-ICD potentially plays a crucial role in the regulation of neuroblastoma cell proliferation.

3.5. NLRR3-ICD stimulates ATRA-mediated neuroblastoma cell differentiation

Since SH-SY5Y cells showed the remarkable ATRA-induced neurite extension accompanied by the massive accumulation of NLRR3-ICD (Fig. 1A), it is possible that NLRR3-ICD has a capability to trigger or enhance neurite elongation in neuroblastoma cells initiated by ATRA. To address this issue, SK-N-BE cells stably expressing the indicated NLRR3 derivatives were exposed to 1.5 μM of ATRA. Five days after treatment, images were taken and then total neurite outgrowth was assessed. As shown in Fig. 4D and E, an obvious increase in number of cells with neurite extension was observed in HA-NLRR3, HA-NLRR3-d-ECD or HA-NLRR3-ICD-expressing cells relative to that in the empty plasmid control cells. In contrast, HA-NLRR3-ECD and HA-NLRR3-ECD-sol did not have a significant effect on ATRA-mediated neurite outgrowth. Similar

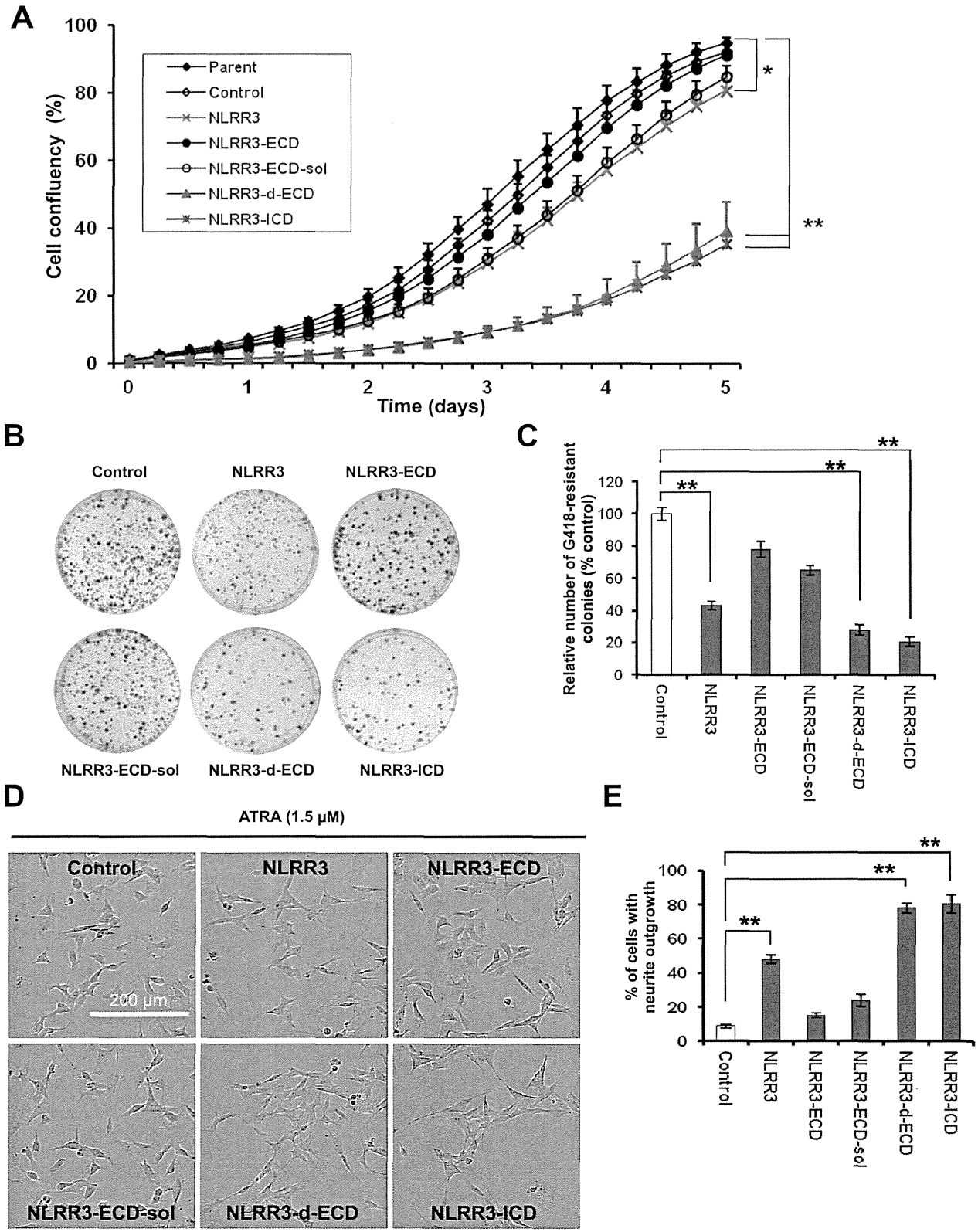

Fig. 4. NLRR3-ICD promotes growth suppression and ATRA-dependent neurite extension of neuroblastoma cells. (A) Growth curves. SK-N-BE cells stably expressing the indicated NLRR3 derivatives were grown in the medium and their growth rates were monitored by IncuCyte. (B and C) Colony formation assay. SK-N-BE cells were transfected with the indicated expression plasmids, and maintained in the culture medium containing 600 μg/ml of G418. Two weeks after the selection, drug-resistant colonies were stained with Giemsa's solution (B) and scored (C). (D and E) NLRR3-ICD enhances neurite elongation in response to ATRA. SK-N-BE cells stably expressing the indicated NLRR3 derivatives were maintained in the culture medium containing 1.5 μM of ATRA for 5 days and their images were taken through phase-contrast microscope. Scale bar; 200 μm (D). Histogram illustrates the percentage of neurite-bearing cells (E).

results were also obtained in the immunostaining experiments using anti-Tuj-1 antibody (Supplementary Fig. S1). Collectively, our present findings strongly suggest that the secretase-mediated proteolytic processing of NLRR3 to generate the COOH-terminal intracellular fragment and its subsequent nuclear access play a pivotal role in the regulation of ATRA-dependent neuroblastoma differentiation.

4. Discussion

It has been well-recognized that the therapeutic approach based on the induced differentiation of tumor cells is one of the most attractive strategies for malignant and aggressive tumor treatment. In this connection, a growing body of evidence demonstrated that retinoids have an ability to induce neuronal differentiation of neuroblastoma [19]. Indeed, ATRA-mediated differentiation of neuroblastoma cells has become a currently used therapeutic protocol. However, a precise molecular basis behind the neuroblastoma differentiation following ATRA exposure has been elusive. In this study, we have found for the first time that NLRR3, which is expressed higher in favorable neuroblastomas relative to unfavorable ones, participates in ATRA-induced neuroblastoma differentiation, and thus our present results might provide a novel insight into understanding ATRA-mediated biological responses such as differentiation.

One of the interesting findings of the present study is that the COOH-terminal intracellular domain of NLRR3 (NLRR3-ICD) is induced to be released from the plasma membrane and then accumulates in cell nucleus during ATRA-dependent differentiation of neuroblastoma SH-SY5Y cells. Indeed, ATRA-mediated nuclear access of NLRR3 in SH-SY5Y cells was massively attenuated in the presence of γ-secretase inhibitor as examined by immunostaining experiments (data not shown), and NLRR3-ICD production was significantly blocked by α- or γ-secretase inhibitor treatment, suggesting that ATRA-induced generation of NLRR3-ICD is regulated at least in part by secretase activities. In accordance with the previous findings showing that there are no distinct consensus amino acid sequences of intramembrane γ-cleavage sites among a broad range of its substrates [16], NLRR3 transmembrane domain also displayed no amino acid sequence similarity to those of Notch as well as the other γ-secretase substrates. However, the transmembrane domain of NLRR3 was highly conserved among human, mouse and rat (Fig. 2A), raising a possibility that γ-secretase-mediated liberation of the intracellular cytoplasmic domain of NLRR3 is evolutionarily conserved across mammalian species.

Meanwhile, it has been well-known that the released NICD directly moves from cytoplasm to nucleus, and then forms nuclear transcription complex with the sequence-specific DNA-binding protein CSL, Mastermind (MAM) family of transcriptional co-activators and/or transcriptional co-repressor MINT to transactivate and/or transrepress Notch-target genes [15]. According to our present observations, the exogenously expressed HA-NLRR3-ICD was translocated to cell nucleus, and also HA-NLRR3-ICD generated in SK-N-BE cells overexpressing HA-NLRR3 was detectable in nuclear fraction. Since we found out a canonical nuclear translocation signal (NLS) within NLRR3-ICD (RNYLQKPTFALGELYPP), it is possible that the nuclear access of NLRR3-ICD might be mediated by this putative NLS. Considering that Notch signaling results in the up-regulation and/or down-regulation of various Notch-target gene expression, it should be critical to investigate whether, like NICD, NLRR3-ICD could form active transcription complexes to regulate its target gene expression implicated in ATRA-mediated neuroblastoma differentiation.

As described [14], NLRR family consists of three members including NLRR1, NLRR2 and NLRR3. The close inspection of their transmembrane domains showed that there is no amino acid sequence similarity among them. Although a biological significance(s) of NLRR2 has remained to be determined, we have demonstrated that, in contrast to NLRR3, NLRR1 is expressed higher in unfavorable neuroblastomas as compared with that in favorable ones, and its expression level is correlated with poor prognosis of patients with neuroblastoma [13]. Subsequent studies revealed that *NLRR1* is a direct transcriptional target of MYCN and has an oncogenic potential [20]. Notably, there existed an inverse relationship between the expression levels of *NLRR3* and *MYCN* during ATRA-mediated neuroblastoma differentiation [14]. In support with this notion, forced expression and siRNA-mediated knockdown of *MYCN* resulted in a massive down- and up-regulation of *NLRR3* expression, respectively [14]. Based on our observations, it is likely that NLRR family such as NLRR1 and NLRR3 stands at the crossroad between MYCN-mediated oncogenic transformation and neuronal differentiation. Further studies should be required to adequately address this issue.

Taken together, our present findings strongly suggest that NLRR3-ICD generated by secretase-mediated proteolytic processing of NLRR3 contributes to ATRA-induced neuroblastoma differentiation, and might provide a clue to develop a novel therapeutic strategy for the treatment of aggressive neuroblastoma based on ATRA-induced differentiation.

Acknowledgments

This work was supported by a Grant-in-Aid from the Japan Ministry of Health, Labour and Welfare for Third Term Comprehensive Control Research for Cancer to A.N., JSPS KAKENHI Grant Number 21390317, 24249061 to A.N., 19890276 to A.T., MEXT KAKENHI Grant Number 22791016 to A.T.

Appendix A. Supplementary data

Supplementary data associated with this article can be found, in the online version, at http://dx.doi.org/10.1016/j.bbrc.2014.09.065.

References

[1] J.M. Maris, Recent advances in neuroblastoma, N. Engl. J. Med. 362 (2010) 2202–2211.
[2] G.M. Brodeur, A. Nakagawara, Molecular basis of clinical heterogeneity in neuroblastoma, Am. J. Pediatr. Hematol. Oncol. 14 (1992) 111–116.
[3] M.J. Cooper, S.M. Steinberg, J. Chatten, A.E. Evans, M.A. Israel, Plasticity of neuroblastoma tumor cells to differentiate along a fetal adrenal ganglionic lineage predicts for improved patient survival, J. Clin. Invest. 90 (1992) 2402–2408.
[4] A. Nakagawara, M. Arima-Nakagawara, N.J. Scavarda, C.G. Azar, B. Cantor, G.M. Brodeur, Association between high levels of expression of the TRK gene and favorable outcome in human neuroblastoma, N. Engl. J. Med. 328 (1993) 847–854.
[5] V.R. Ganeshan, N.F. Schor, Pharmacologic management of high-risk neuroblastoma in children, Paediatr. Drugs 13 (2011) 245–255.
[6] J. Hara, Development of treatment strategies for advanced neuroblastoma, Int. J. Clin. Oncol. 17 (2012) 196–203.
[7] D. Meitar, S.E. Crawford, A.W. Rademaker, S.L. Cohn, Tumor angiogenesis correlates with metastatic disease, N-myc amplification, and poor outcome in human neuroblastoma, J. Clin. Oncol. 14 (1996) 405–414.
[8] J.M. Maris, K.K. Matthay, Molecular biology of neuroblastoma, J. Clin. Oncol. 17 (1999) 2264–2279.
[9] G.P. Tonini, Neuroblastoma: the result of multistep transformation?, Stem Cells 11 (1993) 276–282
[10] R. Ijiri, Y. Tanaka, K. Kato, K. Misugi, H. Nishihira, Y. Toyoda, H. Kigasawa, T. Nishi, M. Takeuchi, N. Aida, T. Momoi, Clinicopathologic study of mass-screened neuroblastoma with special emphasis on untreated observed cases: a possible histologic clue to tumor regression, Am. J. Surg. Pathol. 24 (2000) 807–815.
[11] G. López-Carballo, L. Moreno, S. Masiá, P. Pérez, D. Barettino, Activation of the phosphatidylinositol 3-kinase/Akt signaling pathway by retinoic acid is required for neural differentiation of SH-SY5Y human neuroblastoma cells, J. Biol. Chem. 277 (2002) 25297–25304.
[12] M. Ohira, A. Morohashi, H. Inuzuka, T. Shishikura, T. Kawamoto, H. Kageyama, Y. Nakamura, E. Isogai, H. Takayasu, S. Sakiyama, Y. Suzuki, S. Sugano, T. Goto, S. Sato, A. Nakagawara, Expression profiling and characterization of 4200

genes cloned from primary neuroblastomas: identification of 305 genes differentially expressed between favorable and unfavorable subsets, Oncogene 22 (2003) 5525–5536.
[13] S. Hamano, M. Ohira, E. Isogai, K. Nakada, A. Nakagawara, Identification of novel human neuronal leucine-rich repeat (hNLRR) family genes and inverse association of expression of Nbla10449/hNLRR-1 and Nbla10677/hNLRR-3 with the prognosis of primary neuroblastomas, Int. J. Oncol. 24 (2004) 1457–1466.
[14] J. Akter, A. Takatori, M.S. Hossain, T. Ozaki, A. Nakazawa, M. Ohira, Y. Suenaga, A. Nakagawara, Expression of NLRR3 orphan receptor gene is negatively regulated by MYCN and Miz-1, and its downregulation is associated with unfavorable outcome in neuroblastoma, Clin. Cancer Res. 17 (2011) 6681–6692.
[15] K. Hori, A. Sen, S. Artavanis-Tsakonas, Notch signaling at a glance, J. Cell Sci. 126 (2013) 2135–2140.
[16] B. De Strooper, Aph-1, Pen-2, and Nicastrin with Presenilin generate an active gamma-Secretase complex, Neuron 38 (2003) 9–12.
[17] G.H. Searfoss, W.H. Jordan, D.O. Calligaro, E.J. Galbreath, L.M. Schirtzinger, B.R. Berridge, H. Gao, M.A. Higgins, P.C. May, T.P. Ryan, Adipsin, a biomarker of gastrointestinal toxicity mediated by a functional gamma-secretase inhibitor, J. Biol. Chem. 278 (2003) 46107–46116.
[18] S.E. Hoey, R.J. Williams, M.S. Perkinton, Synaptic NMDA receptor activation stimulates alpha-secretase amyloid precursor protein processing and inhibits amyloid-beta production, J. Neurosci. 29 (2009) 4442–4460.
[19] M. Ponzoni, P. Bocca, V. Chiesa, A. Decensi, V. Pistoia, L. Raffaghello, C. Rozzo, P.G. Montaldo, Differential effects of *N*-(4-hydroxyphenyl)retinamide and retinoic acid on neuroblastoma cells: apoptosis versus differentiation, Cancer Res. 55 (1995) 853–861.
[20] M.S. Hossain, T. Ozaki, H. Wang, A. Nakagawa, H. Takenobu, M. Ohira, T. Kamijo, A. Nakagawara, N-MYC promotes cell proliferation through a direct transactivation of neuronal leucine-rich repeat protein-1 (NLRR1) gene in neuroblastoma, Oncogene 27 (2008) 6075–6082.

日本臨牀　73巻 増刊号1（2015年1月20日発行）別刷

最新肝癌学

—基礎と臨床の最新研究動向—

XV 特　　論

肝芽腫の診断と治療

上條岳彦　　檜山英三

XV 特　論

肝芽腫の診断と治療

Diagnosis and treatments of hepatoblastoma

上條岳彦[1]　檜山英三[2]

Key words：肝芽腫，小児悪性肝腫瘍，JPLT

はじめに

我が国では小児悪性肝腫瘍の治療成績向上のために，グループスタディの開始による治療研究の必要性が検討され，1989年からスタディグループ設立が有志の治療医によって行われ，発起人会の設立，スタディグループ発足の準備が進められた．Société Internationale d' Oncologie Pédiatrique-Epithelial Liver Tumor Study Group(SIOPEL)から日本へ治療研究への参加要請があり検討の結果，日本独自のプロトコール施行と決定され，1991年に日本小児肝癌スタディグループ(Japanese study group for Pediatric Liver Tumor: JPLT)が結成された．治療の詳細は後に記述するが，JPLT-1治療研究が1991-99年まで施行され，次にJPLT-2治療研究が1999-2012年まで施行された．現在は2012年からJPLT-3治療研究に移行し，継続して小児肝悪性腫瘍の治療成績向上が図られている．

1 肝芽腫の疫学

小児の悪性肝腫瘍は，白血病リンパ腫を含めた小児悪性腫瘍全体の約1％といわれている．これは日本における小児悪性固形腫瘍の3-4％に相当する．その大部分は肝芽腫と成人型肝癌である肝細胞癌である．小児の肝腫瘍にはこのほかにも肝未分化胎児性肉腫のような比較的まれな悪性腫瘍や，血管腫，巣状結節性過形成のような良性腫瘍がある．小児の悪性肝腫瘍は，小児肝腫瘍のおよそ6割を占める．

小児肝細胞癌は小児の悪性肝腫瘍の10-30％を占めるとされている．チロシン血症，胆道閉鎖症，新生児肝炎，α1-アンチトリプシン欠損症，栄養性およびウイルス性肝硬変などの慢性的な病気からの肝細胞癌が報告されている．

肝芽腫は最も多い小児の悪性肝腫瘍であり，その年間発症数は40-50例と考えられている．肝芽腫の危険因子としては，我が国から低出生体重児と肝芽腫発症の相関が報告されている．出生体重2,500グラム以上の正常体重児と比較して，<1,000，1,000-1,499，1,500-1,999，and 2,000-2,499の児の相対危険度(relative risk)はそれぞれ15.64(p<0.001)，2.53(p=0.129)，2.71(p=0.001)，and 1.21(p=0.381)となっていた[1]．

ほかの肝芽腫の危険因子として，幾つかの先天症候群や疾患が知られている．Beckwith-Wiedemann症候群，家族性大腸腺腫症，糖原病(I～IV型)，18トリソミーなどである．Beckwith-Wiedemann症候群は巨舌，腹壁欠損(臍帯ヘルニア，腹直筋解離，臍ヘルニア)，過成長を三主徴とする先天奇形症候群である．約15

[1]Takehiko Kamijo, [2]Eiso Hiyama: [1]Research Institute for Clinical Oncology, Saitama Cancer Center　埼玉県立がんセンター　臨床腫瘍研究所　[2]Natural Science Center for Basic Research and Development, Hiroshima University　広島大学　自然科学研究支援開発センター；Hiroshima University Hospital, Pediatric Surgery Department　広島大学病院　小児外科

0047-1852/15/¥60/頁/JCOPY

%の症例で肝芽種，横紋筋肉腫，Wilms腫瘍など胎児性腫瘍が発生する．本症候群の原因遺伝子座は11番染色体短腕15.5領域（11p15.5）で，この領域には多くの刷り込み遺伝子がクラスターを形成して存在する．本症候群は，11p15.5の刷り込み異常によって生じる．11p15.5には，2つの刷り込みドメイン，KIP2/LIT1ドメインとIGF2/H19ドメインがあり，それぞれ刷り込み調節領域により周辺の刷り込み遺伝子の発現が制御されている．本症候群の10％はIGF2/H19ドメインのH19DMR高メチル化によるIGF2の発現上昇によって発症する（難病情報センターサイト改変）．さらに11p15.5部位のLOHが3/13の肝芽腫症例でみられ，また同部位のインプリンティングが5例の肝芽腫で報告されている[2]．以上から，IGF2増加はBeckwith-Wiedemann症候群と肝芽腫発症に関連があると想定されている．

家族性大腸腺腫症と肝芽腫の間には関連がみられることが知られている[3]．家族性大腸腺腫症の家族歴をもつ場合，肝芽腫の発生リスクが800倍上昇することが知られている．肝芽腫に関連するadenomatous polyposis coli（APC）遺伝子変異は，典型的な家族性大腸腺腫症関連遺伝子変異と多少異なり，1309番塩基近傍のAPC遺伝子N末端側に多く位置するといわれている．肝芽腫症例でAPC遺伝子生殖細胞変異が認められない場合，肝芽腫のAPC遺伝子体細胞変異はみられないが，APC下流分子として知られるβカテニン遺伝子に変異が認められる傾向があることが知られている．これは孤発性肝芽腫の48％に及ぶものであり，βカテニン遺伝子のエクソン3に変異が認められ，βカテニン分子の分解を阻害する変異であった．

2 上記以外の肝芽腫のゲノム・エピゲノム異常

我が国において56例の肝芽腫症例に対してSNIPアレイを用いた解析を行い，アレル不均衡が37例（66％）で見いだされた．染色体のゲインが1q（28サンプル），2q（24），6p（8），8q（8），17q（6），および20pq（10）で，染色体のロスが1p（6サンプル），4q（9）および16q（4）で認められた．特に1q32.1においては癌遺伝子MDM4の増幅がみられた腫瘍が存在した[4]．

また我が国のJPLT-2プロトコール症例74例の解析結果，25例（33.8％）に癌抑制遺伝子RASSF1Aプロモーター部位のゲノムメチル化が見いだされ，転移および不良な予後との相関が示された[5]．

3 肝芽腫の臨床像

肝芽腫の症状としては，孤発例では腹部膨満，腹部腫瘤触知などが多く，早期の発見は難しい．基礎疾患が先行する場合には，肝芽腫発症リスクを考慮してのフォローアップの経過で発見される（Beckwith-Wiedemann症候群など）．発見時にかなり進行している例もみられるため，発育遅延，体重増加停止などの全身症状が認められることもある．また転移した部位においての病変形成によって症状が認められる（肺転移，下大静脈・門脈転移など）．

4 肝芽腫の検査

1）生化学的検査

肝芽腫ではほとんどα-フェトプロテイン（AFP）は陽性であり，かつ極めて高値を示すことが多い．AFPは胎児期肝細胞などにより産生されるタンパクであり，出生後に産生されなくなるが，満期産児では10,000-100,000 ng/mLと高値である．半減期は4-9日であり，生後6カ月で50 ng/mL，生後1年で20 ng/mL以下と成人レベルに低下する．診断時のAFP値は年齢で調整した正常範囲と比較されるべきである．診断時のAFPレベルと臨床予後の関連については，100 ng/mLのものは未分化小細胞型が多く予後不良との報告があるが，我が国では極めてまれである．一方で，血清AFPレベルは治療反応性の優れた指標として用いられている．ドイツ小児癌治療グループのHB-89プロトコールでは，化学療法時の血清AFPの減少が予後と

明らかに相関していた(p=0.003)[6].

Children's Cancer Group(CCG) protocol 823Fの結果から，化学療法などの治療を行っても血清AFPレベルが低下しない場合には，治療に対する反応性の低下が想定される．他の検査値ではLDHの高値，また乳児性肝絨毛癌ではβ-hCG腫瘍マーカーの高値が認められる．

2) 治療前に施行されるべき検査

肝芽腫治療では後述する化学療法が施行されるが，小児に化学療法を行う場合，晩期合併症として幾つかの頻度の高い合併症が知られており，程度・経過を把握するために治療前の評価が望ましい．

聴力検査(オージオメーターでの測定)：シスプラチン・カルボプラチンなどの抗癌剤の副作用として聴力の低下が報告されているため，治療前の聴力を検査する．治療中は定期的に聴力を測り，聴力低下の有無を確認する．

心機能検査(心エコー・心電図)：THP-アドリアマイシンの副作用として急性・慢性の心筋障害が出現することがあるため，治療前の心機能を評価する．

腎機能検査(尿検査)：シスプラチンの副作用で腎機能障害が発生することがあるために事前に評価する(尿量，BUN，Cre，24hCCr，尿中低分子量タンパクのβ2-MG，腎尿細管酵素NAG，血清電解質など)．

3) 画像検査

肝芽腫の術前画像診断としては，腹部エコー，CT scan，MRIなどによる評価が必要になり，これらを基にPRETEXT分類が検討される．

JPLTプロトコールでは，診断クオリティの担保と治療効果判定のため，診断時，化学療法の経過中に中央判定を施行している．画像はJPLTの診療検討委員会および肝切除・肝移植検討委員会にて検討され，コメントが返送される．

4) 病理学的検査

組織学的には，低分化から未熟型の上皮成分からなる上皮型と，上皮成分と紡錘型異型細胞や軟骨組織などの間葉成分からなる混合型の2つに大別される．鑑別診断にはサイトケラチンやvimentin，S-100タンパクなどの免疫染色が有用とされる．

上皮型はさらに胎児型(fetal type)，胎芽型(embryonal type)，大索状型(macrotrabecular type)，未分化小細胞型(small cell undifferentiated type)に細分される．組織系と予後の関連については，上皮型と混合型の間の予後には有意な差がないとされている．また腫瘍が完全に摘出された場合に純胎児型(pure fetal type)は予後良好であるが，一方で，未分化小細胞型の患者がより不良な予後を示した報告がなされている．現在のJPLT登録症例の病理組織分類は，国際小児肝がん組織分類に基づいて行う．小児腫瘍専門病理医はその人数も限られており，専門病理医によるセントラル・レビューを行う必要がある．'小児固形腫瘍観察研究(事務局　国立成育医療研究センター　病理診断部)'に登録している施設のJPLT症例は，中央病理診断が施行されている．

5 肝芽腫の臨床病期分類

肝芽腫の臨床病期分類は，切除性を重視した術後病期分類と治療前の進展度による術前病期分類が用いられている(小児肝がん　臨床ガイドライン)．Société Internationale d' Oncologie Pédiatrique(SIOP)では治療前の進展度によるPretreatment Extent of Disease System (PRETEXT)分類が使用されている[7]．日本では当初日本小児外科学会の病期分類が用いられていたが，JPLT-2プロトコール以降はPRETEXT分類が採用されている．これは肝臓全体を4つに分けた区域(4区域)のそれぞれにおける腫瘍の拡がりの有無(MRIやCTなどの画像検査法によって判定される)を基準とした病期分類である(**図1**)．

JPLTではJPLT-2プロトコールに対して1999年から2008年12月までに279例の小児悪性肝腫瘍が登録され，このうち212例が肝芽腫と診断された．この212例の病期と治療成績は，PRETEXT分類I(16例)，II(64例)，III(83例)，IV(49例)の5年生存率はそれぞれ93.8%，84.4%，86.1%，63.2%であった[8]．

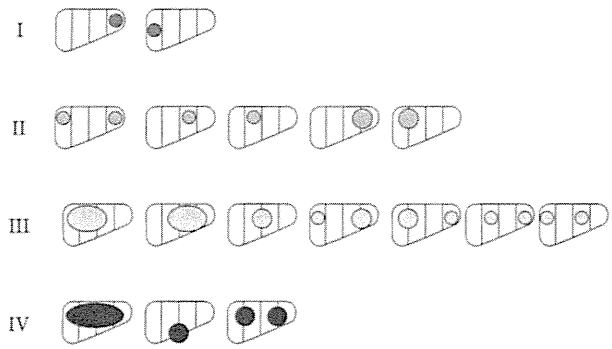

PRETEXTのほかに，下の4つの『肝外進展』と『遠隔転移』の有無を確認して治療を行う．
V→下大静脈またはすべての肝静脈内へ腫瘍が入り込んでいる場合．
P→門脈本幹，または左右両方の門脈内に腫瘍がある場合．
E→VやP以外の肝外進展がある場合．
R→腫瘍破裂がある場合．
F→多発性腫瘍の場合．
M→遠隔転移がある場合．

PRETEXT分類I	腫瘍は1つの肝区域に存在し，他の隣接する3区域に腫瘍の浸潤を認めない
PRETEXT分類II	腫瘍は2つの肝区域に存在し，他の隣接する2区域に腫瘍の浸潤を認めない
PRETEXT分類III	腫瘍は2つ以上の隣接しない肝区域または3つの隣接する肝区域に存在し，他の1区域あるいは隣接しない2区域に腫瘍の浸潤を認めない
PRETEXT分類IV	腫瘍は4つの肝区域に存在する

図1 PRETEXT分類法（図示）

6 海外での臨床試験の実態

1980年代までは，肝芽腫の治療は外科療法が主体であり，その生存率は全体で20–30％と良好な成績ではなかった．1970年代のシスプラチン（CDDP）の開発に伴い，1980年代後半からCDDPとドキソルビシン（DOX）を中心とした化学療法が用いられ，治療成績が向上した．

SIOPが初めて行った小児肝悪性腫瘍の国際的臨床試験がSIOPEL–1である．SIOPEL–1は1990–94年に194症例（肝芽腫154例，肝細胞癌40例）に対して施行され，CDDP/DOX療法による術前化学療法の有効性を検証した[9]．これは術前にCDDP（80 mg/m^2，24時間持続静注）とDOX（30 mg/m^2，24時間持続静注，day2とday3，total 60 mg/m^2）を4クール行い，術後に2クール追加するプロトコールであった．5年無イベント生存期間（EFS）と全生存期間（OS）はそれぞれ66％と75％であり，従来の治療から顕著な改善がみられた．このSIOPEL–1プロトコールによってCDDP/DOX療法による術前化学療法の有効性が示され，また治療前に腫瘍が占める肝臓の区域による分類（PRETEXT）と肺転移の有無が生存期間と無病生存期間に相関していることが示された[7]．

これらを基にSIOPEL–2プロトコールとして，CDDP単独療法（80 mg/m^2，24時間持続静注，4クールを2週間ごとに行い，術後に2クール追加）を標準リスク群77例，高リスク群58例に対して1995–98年に施行した．標準リスク群では3年EFSとOSはそれぞれ89％と91％であり，良好な成績が得られた．高リスク群では3年EFSとOSはそれぞれ48％と53％であった[10]．

1998年から2006年に行われたSIOPEL–3ではCDDP単独療法のCDDP/DOX療法に対するランダム化非劣性試験が行われ，CDDP単独療法126例とCDDP/DOX療法129例が解析され，CDDP単独療法の3年EFSとOSはそれぞれ83％と95％，CDDP/DOX療法の3年EFSとOSはそれぞれ85％と93％でCDDP単独療法の非劣性が示された[11]．

その後高リスク肝芽腫に対するSIOPEL–4プロトコールが2005年からスタートし，術前のCDDP/DOX療法を3コース後に術前にcarboplatin/DOX療法を1コース行い手術の1アームと，術前のCDDP/DOX療法を3コース後に手術，術後にcarboplatin/DOX療法を1コース行う1アームのどちらかを行う治療が2009年まで行われた．

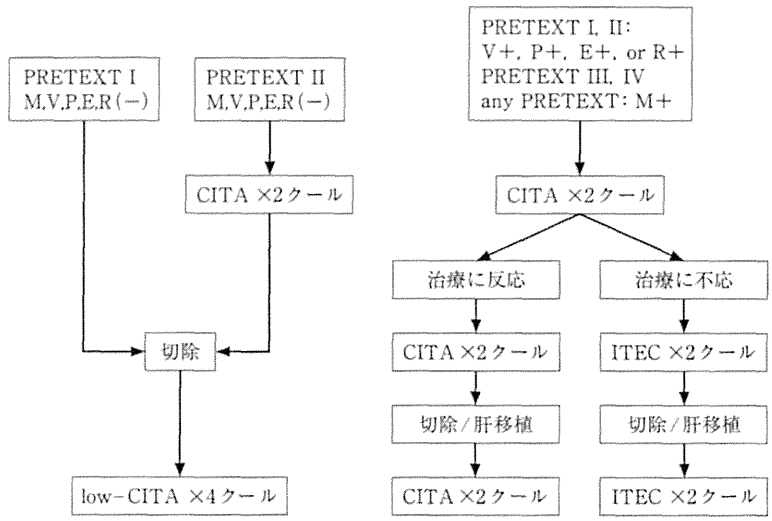

図2 JPLT-2プロトコールの概略図

米国でもヨーロッパと同様に肝芽腫に対するChildren's Cancer Groupが施行したCDDP/DOX療法[12]，Pediatric Oncology Groupが施行したCDDP/VCR/5-FU療法[13]などによって化学療法の有効性が証明されてきた．その後米国ではCCG，POGなどの統合によるChildren's Oncology Groupがスタートし，現在COG-AHEP0731(Combination Chemotherapy in Treating Children With Newly Diagnosed Hepatoblastoma)が施行されている．

7 国内の臨床試験の歴史

まずJPLT-1プロトコールが1991-99年まで行われた．これはCDDPと我が国開発のピラルビシン(THP-ADR)を併用したCITA療法を行うものである．病期IとII症例にはCDDP 40 mg/m²とTHP-ADR 30 mg/m²を投与し，病期IIIA，IIIBとIV症例にはCDDP 80 mg/m²とTHP-ADR 30 mg/m²×2 daysを投与するものであり，それぞれ手術前後に計6コース行われた．登録154例の小児悪性肝腫瘍中，145例が肝芽腫であり，全生存率は(3-year/6-year)，病期I(n=9)が100 %/100 %，病期II(n=32)が100 %/95.7 %，病期IIIA(n=48)が76.6 %/73.8 %，病期IIIB(n=25)が50.3 %/50.3 %，病期IV(n=20)が64.8 %/38.9 %であり，全体では77.8 %/73.4 %であった．これは当時のヨーロッパのSIOPEL-1プロトコール，および米国のINT-098プロトコールとほぼ同等の成績であった[14]．

JPLT-1プロトコールでは，肝臓の4区域を占める病期IIIB症例の完全切除率は55 %と高くなく，手術不能例における無病生存例はいなかった．一方，病期I，IIの症例では欧米より抗癌剤使用量が少ないにもかかわらず，OSは90 %以上と良好であった．

よって，次期のJPLT-2プロトコールでは，早期例の治療軽減による副作用の減少と，進行例の術前化学療法強化による治療成績の向上が図られた．

JPLT-2プロトコールにおいては，化学療法として，①low-CITA療法(CDDP 40 mg/m²とTHP-ADR 30 mg/m²)，②CITA療法(CDDP 80 mg/m²とTHP-ADR 30 mg/m²×2 days)，③ITEC療法(イフォマイド：IFO，カルボプラチン：CBDCA，エトポシド：VP-16，THP-ADR)を**図2**に示すように各症例に対して施行した．また一部の症例に対しては，CATA-L療法(THP-ADR 30 mg/m²とCBDCA 200 mg/m²による肝動脈化学塞栓療法)を施行した．

悪性小児肝腫瘍389例，うち肝芽腫331例が

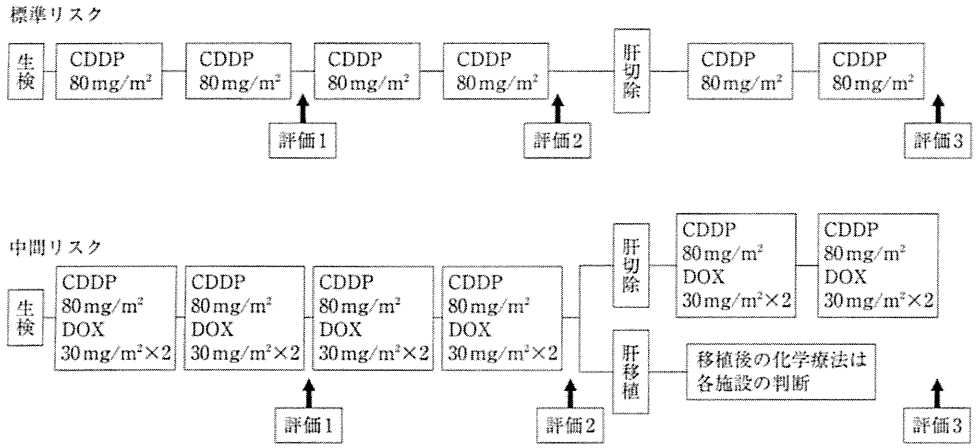

図3　JPLT-3プロトコール概略
評価は血清AFP値および画像評価（US，CT，必要に応じMRI）を行う．

2010年までに登録された．5年生存率と5年無病生存率はそれぞれ83.3％と68.0％であった．低リスク例の患者の予後は良好であったが，高リスク例（肝4区域進展例および遠隔転移例）の予後は不良であった．暫定解析での5年生存率は転移なしの群でfor PRETEXT I: 100％，PRETEXT II: 87.1％，for PRETEXT III: 89.7％，PRETEXT IV: 78.3％であった．一方転移例の5年生存率は43.9％であった[15]．以上の結果から，低リスク例でのCITA療法の有効性は確認され，転移例ではCITA療法，ITEC両方とも十分な有効性は得られなかった．CATA-L療法は施行例数が十分でなく有効性は証明できなかった．また，二次癌，特に二次性と考えられる白血病が5例生じ，これは高頻度と考えられる．THP-ADR使用との関連などを検討する必要があると思われている．

8　国内の臨床試験の現状

JPLT-1およびJPLT-2プロトコールの成績を基に，JPLT-3プロトコールでは様々な変更点が立案された．

まずリスク分類については，SIOPEL（ヨーロッパ）あるいはCOG（米国）のリスク分類を受けて，以下の国際リスク分類を採用した．これは国際小児肝癌共同研究（Children's Hepatic Tumor International Collaboration: CHIC）によって開発されている包括的な研究への参加・協力を図ることから採用された．

［国際リスク分類］

（1）高リスク（以下のいずれかの患者）

血清AFP＜100 ng/mL

PRETEXT付記因子：M1（転移臓器問わず），N2（遠隔リンパ節転移）

（2）中間リスク（以下のいずれかの患者，高リスク例は除外）

PRETEXT IV

PRETEXT付記因子で以下の因子を1つ以上満たすもの

E1，E1a，E2，E2a

H1，N1

P2，P2a

V3，V3a

多発（腫瘍が2カ所以上肝内に存在する）

診断時年齢が3歳以上

初診時肝破裂例

（3）標準リスク例（上記（1），（2）以外の患者）

JPLT-3プロトコールの概略を**図3**に示す．標準リスク例に対しては試験治療（CDDP単剤療法）が，JPLT-2プロトコールにおけるCITA療法（CDDP+THP-ADR）と同様に有効であるかを判定する．標準リスク例は年間15-20例と推定され，必要症例数は75例と推測され，これ